PIBB 生物化学与生物物理进展
*Progress in Biochemistry and Biophysics*
2020,47(2):139~156
www.pibb.ac.cn

# Alteration of Neural Activity in The Sensorimotor and Visual Cortices and Vigilance Level During Sleep Deprivation*

ZHANG Dai[1,2], ZUO Zhen-Tao[3,4,5)**], RAO Heng-Yi[6)], FAN Yong[7)**]

([1)]*National Laboratory of Pattern Recognition, Institute of Automation, Chinese Academy of Sciences, Beijing* 100190, China;
[2)]*University of Chinese Academy of Sciences, Beijing* 100049, China;
[3)]*State Key Laboratory of Brain and Cognitive Science, Institute of Biophysics, Chinese Academy of Sciences, Beijing* 100101, China;
[4)]*Sino-Danish College, University of Chinese Academy of Sciences, Beijing* 100049, China;
[5)]*CAS Center for Excellence in Brain and Science and Intelligence Technology, Chinese Academy of Sciences, Shanghai* 200031, China;
[6)]*Department of Neurology, Perelman School of Medicine, University of Pennsylvania, Philadelphia, PA* 19104, USA)
[7)]*Department of Radiology, Perelman School of Medicine, University of Pennsylvania, Philadelphia, PA* 19104, USA)

**Abstract** The mechanism underlying the alteration of neural activity in the human brain and the vigilance level during sleep deprivation (SD) remains a subject of ongoing investigation, particularly with regard to the sensorimotor and visual systems. Resting-state functional magnetic resonance imaging (rfMRI), a noninvasive imaging technology reflecting spontaneous activity of the human brain, is widely used in SD research. In the present study, nine repeated rfMRI sessions followed by a psychomotor vigilance task (PVT) were used to explore the alteration of neural activity and vigilance level during 36 h of SD in 23 volunteers. Mean reaction time (MRT) and lapse ratio (LR) based on PVT were measured to assess variation in vigilance level. The sensorimotor network (SMN) and visual network (VN) are the most vulnerable areas after obtaining SD measures from ReHo (regional homogeneity) and ALFF (amplitude of low-frequency fluctuation) based on rfMRI. Group-ICA was used to parcellate the visual-related regions into visual area I, visual area II, and the visual association area. Sensorimotor-related regions, including the bilateral precentral/postcentral gyrus, the bilateral paracentral lobule, and the supplementary motor area (SMA), were extracted from the anatomical automatic labeling (AAL) templates. Brain neural activity and vigilance level were deteriorated at 16−30 h of SD. A 2 × 3 repeated-measures ANOVA was used to explore the effects of sleep pressure and circadian rhythm and their interaction on neural activities of sensorimotor-related and visual-related regions. Significant effects of sleep pressure and interaction on all sensorimotor-related and visual-related regions were observed. Pearson's correlation coefficients were used to explore the relationships between variation in vigilance level and alteration in brain neural activities of sensorimotor-related and visual-related regions. Significant correlations were observed between the neural activities of all sensorimotor-related regions and variation in vigilance during SD. Our results confirmed that SD alters the vigilance level and neural activity of the SMN and the VN, beginning at 24:00 on the first day, and sleep pressure and circadian rhythm regulate the neural activity of the SMN and VN during SD. Furthermore, sleep pressure significantly regulates the effects of circadian rhythm. The enhancement of ReHo in the SMN and VN leads to a weakening of their remote connections, which may be the cause of the slowing of response time during SD.

**Key words** resting-state fMRI, sleep deprivation, sensorimotor cortex, visual cortex, brain neural activity
**DOI**: 10.16476/j.pibb.2019.0055

* This work was supported by grants from National Basic Research Program of China (2015CB856400, 2015CB351701), The National Natural Science Foundation of China (81501158, 31730039, 31671133), The National Major Scientific Instruments and Equipment Development Project (ZDYZ2015-2), and The Chinese Academy of Sciences Strategic Priority Research Program B grants (XDBS32000000).
** Corresponding author.
ZUO Zhen-Tao . Tel: 86-10-64888462, E-mail: ztzuo@bcslab.ibp.ac.cn; FAN Yong. Tel: 86-215-7464065, E-mail:yong.fan@ieee.org
Received: March 22, 2019 Accepted: April 30, 2019

Sleep is a physiological necessity for normal life, and we spend approximately one-third of our life sleeping. Sleep disorder, which is widespread in the current society, exhibits detrimental effects on the brain function and behavioral performance, such as sensorimotor activity[1-2], visual information processing[3-5], emotional regulation[6-7], working memory[8-9], vigilance level[10-11], and executive control function[12-13]. Sensorimotor and visual activities are two important brain functions that are essential to sustain normal life. Previous research has shown that the adaptation of sensorimotor coupling is impaired by sleep deprivation (SD)[1,14], that SD leads to slower sensorimotor activity and prolonged response time [15], and that the speed of visual information processing is impaired by SD[3], indicating that the functions of the sensorimotor and visual cortices are substantially affected during SD. Circadian rhythm signaling is a fundamental property of the human physiology that is important for sustaining both brain neural activity and essential body functions. A large set of cortical areas, which involves almost the entire cortical mantle, particularly the sensorimotor and visual cortices, are simultaneously affected by the sleep pressure and circadian rhythm signaling during SD[16-18]. The mechanism underlying the alteration of the neural activity in the human brain and the vigilance level during SD remains a subject of ongoing investigation.

Resting-state function magnetic resonance imaging (rfMRI), a noninvasive technology that produces images based on blood oxygen level, can measure the spontaneous activity level of the brain and is widely used disease diagnosis and brain functional mechanism research[19-20]. Several recent studies have used rfMRI to explore the mechanism *via* which spontaneous brain activity and functional connectivity patterns are altered during SD[21-23]. The results suggested that the internal brain activity and interconnectivity patterns are disturbed during SD. Furthermore, the local modulation of human brain responses was affected by sleep pressure and circadian rhythms and the interaction between them[18,24]. These single-time-point SD studies primarily compared rested waking (RW) status with SD status after 24 h of SD and assessed the effect of SD at one specific moment of the circadian rhythm[9,21,25], ignoring the effects of circadian rhythm during SD. One study has evaluated the circadian modulation of the brain response using task-based fMRI (psychomotor vigilance task (PVT) and n-back task) [18]. This design may involve only the brain regions associated with specific tasks. The mechanisms via which the spontaneous activities of the human brain are affected during the entire SD procedure remain unclear, and this led us to investigate the effects of SD procedure at multiple moments of the circadian rhythm.

Based on rfMRI, regional homogeneity (ReHo) and the amplitude of low-frequency fluctuation (ALFF) methods have been used to analyze the alterations of neural activity during the SD procedure[26-27]. ReHo measures the local functional coherence between a given voxel and its neighbors; a larger ReHo indicates higher local field potential synchronization of a given voxel[28]. ALFF measures the low-frequency amplitude of the neurons in the brain that could be employed to evaluate the intensity of intrinsic or spontaneous neuronal activity of the brain. ReHo and ALFF can serve as sensitive markers indicating alterations in brain function. Both ReHo and ALFF have widely been applied to neuropsychiatric disorders and cognitive functions research. For example, ReHo of the inferior frontal cortex and the default mode network (DMN) was significantly correlated with response inhibition ability[29], and ALFF was used to investigate the alterations in regional cortical brain activity in healthy subjects following SD[30]. However, studies exploring the process underlying the changes observed in ReHo and ALFF based on rfMRI, which reflect the spontaneous cerebral activity of the entire brain, during the entire SD procedure are lacking.

PVT, which measures the speed of response to a visual stimulus, is a sustained-attention, reaction-timed task that is widely used because of its ease of scoring, simple metrics, and convergent validity[31]. It is a high signal-load reaction time test that is extremely sensitive to SD, thereby making it one of the leading paradigms used as an assay of vigilant attention. Several studies have applied PVT to assess variation in vigilance attention during SD[32-33]. However, there is a lack of evidence for the relationship between alterations in neural activity and those in vigilance level during SD.

In the present study, a 36 h SD procedure was applied in 23 healthy volunteers. Nine repeated rfMRI sessions followed by a PVT task were used to explore

alterations of neural activity and those of vigilance level during the entire 36-h SD procedure. ReHo and ALFF based on rfMRI were used to investigate variation in spontaneous cerebral activity throughout the entire brain. Subjects' vigilance level was evaluated by their performance in a PVT, including the mean reaction time (MRT) and lapse ratio (LR). To understand the mechanisms of the sensorimotor and visual cortices in the brain during SD, we assessed the relative contributions of circadian rhythms, sleep pressure, and their interaction to alterations in neural activity of the sensorimotor and visual cortices. Furthermore, to explore the physiological evidence for a decline in vigilance level, we evaluated the relationship between variation in the neural activity of the sensorimotor and visual cortices and variation in vigilance level during SD using correlation analysis.

## 1 Materials and methods

### 1.1 Subjects and materials

The present study included 23 healthy volunteers [12 males; (mean± standard deviation) age, (21.7 ± 2.4) years] participated in the present study. All subjects met the following criteria: right-handed; no history of neurological or psychiatric disorders; good sleep habits, without any symptoms of sleep disorders according to the bracelet monitoring of physiological indicators for 1 month before scanning; bedtime at 23: 00 ± 1 h; and regular dietary habits, with moderate weight and body shape. Written informed consent was obtained from each participant, and the study was approved by the Institutional Review Board of the Institute of Biophysics. Three subjects were removed from the study owing to excessive head movements (> 3 mm), and another three subjects were removed owing to missing behavioral data for some sessions.

The experimental protocol consisted of nine MRI scanning sessions for each volunteer over a period of 4 days (Figure 1). The volunteers arrived in the laboratory on the afternoon of the first day, practiced the experimental paradigm, and rested as usual in a scheduled hotel that night. The SD procedure lasted for 36 h from the morning of the second day (8:00) to the evening of the third day (20: 00). The nine MRI scans occurred over the entire 36-h SD procedure. After the ninth MRI scan, the volunteers took a 12-h recovery sleep. The PVT indicators were immediately measured after each MRI scan[31]. The PVT is a simple task, requiring the subject to push a button as soon as the timer appears in the center of the screen. The PVT was randomly conducted every few seconds for 6 min. The reaction time for each trial was recorded. The volunteers were allowed to rest in a meeting room when they were not undergoing MRI and PVT. Food and water were provided during the SD procedure. The temperature of the room was maintained between 23℃ and 27℃ . The volunteers were allowed to read magazines or play chess to ensure that they did not fall asleep. Each volunteer was accompanied by two experimenters during the entire SD procedure. Vigorous exercise was not allowed. The volunteers were not provided information about the time during SD.

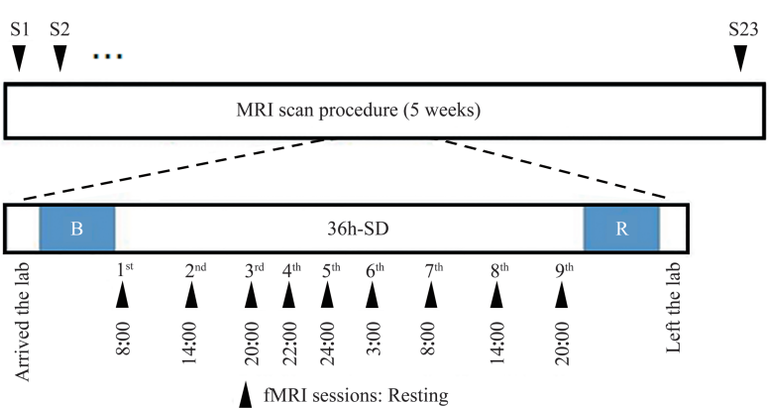



**Fig. 1 Schematic representation of the experimental protocol**

All SD data were recorded during 5 weeks in the laboratory. The entire experimental protocol consisted of nine MRI scanning sessions for each volunteer. After a baseline night （B）, the first to the ninth MRI scans were performed over the entire 36 h SD procedure. After the ninth MRI scan， each volunteer took a 12 h recovery sleep（R）.

### 1.2 MRI data acquisition

MRI data were obtained by a 3.0 Tesla Siemens Prisma$^{fit}$ scanner (Seimens Healthnieer, Erlagen, Germany) located at the National Center for MRI Brain Mapping in the Institute of Biophysics, Beijing. For each MRI session, a high-resolution 3D anatomical image was acquired with T1-weighted MPRAGE: TR = 2 300 ms, TI = 1 600 ms, TE = 3.05 ms, thickness = 1 mm, gap = 0 mm, acquisition matrix = 256 × 256, flip angle = 8°, field of view = 224 mm × 224 mm; and with T2 SPACE image: TR = 3 000 ms, TI = 1 600 ms, TE = 300 ms, acquisition matrix = 256 × 256, field of view= 224 mm×224 mm. Thereafter, rfMRI was acquired using 8min multiband Echo Planar Imaging (EPI): TR = 1 000 ms, TE = 33 ms, thickness = 2.0 mm, gap = 0 mm, acquisition matrix = 96 × 96, flip angle = 45°, field of view = 192 mm × 192 mm, and multiband factor = 4[34]. During the resting state, the subjects were instructed to remain still and awake with their eyes open and focused on a fixation cross during the scan.

### 1.3 Data preprocessing

Preprocessing was performed using the statistical parametric mapping (SPM8) software (http://www.fil.ion.ucl.ac.uk/spm/software/spm8/), the Analysis of Functional NeuroImage technique (AFNI, http://afni.nimh.nih.gov/afni), and the FMRIB Software Library (FSL, http://fsl.fmrib.ox.ac.uk/fsl). To facilitate magnetization equilibrium, the first 10 volumes of the functional images were discarded. Head motion correction was performed by realigning all consecutive volumes to the middle volume (MCFLIRT). Global 4D mean intensity normalization was performed. ICA-AROMA [35], an automated tool for motion artifact removal that is available from the FMRIB Software Library package (FSLv5.0, available athttp://fsl.fmrib.ox.ac.uk/fsl/), was used to enhance the sensitivity and specificity of rfMRI activation and connectivity analyses. In the first step, a probabilistic independent component analysis was run using MELODIC with automatic dimensionality estimation to determine a set of components for each subject per session and per individual recording. Subsequently, components that represented motion-related artifacts were identified (by assessing each component for its high-frequency temporal content, correlation with realignment parameters, and spatial content in the cerebrospinal fluid and edge voxels). Finally, motion-related components were regressed out of the data. To obtain results at the group level, the single-subject images were nonlinearly normalized to Montreal Neurological Institute space using DARTEL of SPM8 and resampled to 3 × 3 × 3 mm$^3$ voxels. Then, temporal bandpass filtering (0.01 Hz< $f$ < 0.08 Hz) was performed to reduce low-frequency drift and physiological high-frequency respiratory and cardiac noise.

MRT and LR were extracted from each PVT run to assess the subject's vigilance level. MRT in a single PVT run was defined as the mean response time for all reaction trials. LR in a single PVT run was defined as the number of trials with reaction time >500 ms divided by the total number of reaction trials. In the subsequent analysis, to assess variation in vigilance level during SD, the average variation of MRT and LR across three contrasts of the 24 h SD procedure (8:00 contrast, comparing the seventh with the first session; 14:00 contrast, comparing the eighth with the second session; and 20:00 contrast, comparing the ninth with the third session) was calculated.

### 1.4 Calculation of ReHo and ALFF

ReHo and ALFF based on rfMRI were applied to explore variation in spontaneous cerebral activity throughout the entire brain during the 36 h SD procedure. The ReHo map and ALFF map were calculated for each individual within a gray matter mask. ReHo was defined by Kendall's coefficient of concordance, which was used to measure ReHo of the time series of a given voxel with the neighbor voxels[26]. A larger ReHo value for a given voxel indicates a higher local synchronization of rfMRI signals among neighboring voxels. The ReHo maps were smoothed using an 8 mm full width at half maximum (FWHM) Gaussian kernel.

ALFF evaluates the amplitude of spontaneous fluctuations of certain voxels in the resting-state brain[27,36]. First, the time series of each voxel were converted to a frequency domain using a Fast Fourier Transform. The ALFF map was defined by the square root of the power spectrum within the frequency range between 0.01 Hz and 0.08 Hz of each voxel. A greater ALFF value for a particular voxel indicates that this voxel exhibits a higher neuron activity level. The ALFF maps were smoothed using an 8 mm FWHM Gaussian kernel.

Calculation of ReHo and ALFF was performed with AFNI (http://afni. nimh. nih. gov/afni). In the subsequent correlation analysis, to assess variation in brain neural activity during SD, variation in ReHo and ALFF was defined as the average variation of ReHo and ALFF across three contrasts of the 24 h SD procedure, which was similar to the previous calculation of the variation of vigilance level during SD.

### 1.5　Definitions of visual−related regions and sensorimotor−related regions

The visual network (VN) regions were extracted by multisession temporal concatenation ICA (TICA) with MELODIC (FSL, http://fsl. fmrib. ox. ac. uk/fsl). All rfMRI data were concatenated through the time dimension, represented as a 2D time × space matrix. Further, MELODIC decomposed this matrix into pairs of time courses and spatial maps. Three space components (visual I, visual II, and visual association area) of the VNs were extracted by artificial check (Figure 2). The visual association area plays a primary role in the recognition of complex patterns, such as images of objects, abstract forms, hands, faces, or even specific faces, whereas the primary visual cortex (visual I and visual II) is essential for detecting basic visual features: light and dark, location, etc.[37]

The sensorimotor network (SMN) regions include somatosensory (postcentral gyrus) and motor (precentral gyrus) regions and extends to the supplementary motor areas [38]. These sensorimotor subregions may be involved in a premediated state that prepares the brain for performing and coordinating a motor task [39]. The paracentral lobule (PCL) is the continuation of the precentral and postcentral gyri and controls motor and sensory innervations of the contralateral lower extremity. Hence, the SMN regions include the precentral gyrus, the postcentral gyrus, the PCL, and the supplementary motor area (SMA) that were extracted from the anatomical automatic labeling (AAL) template.

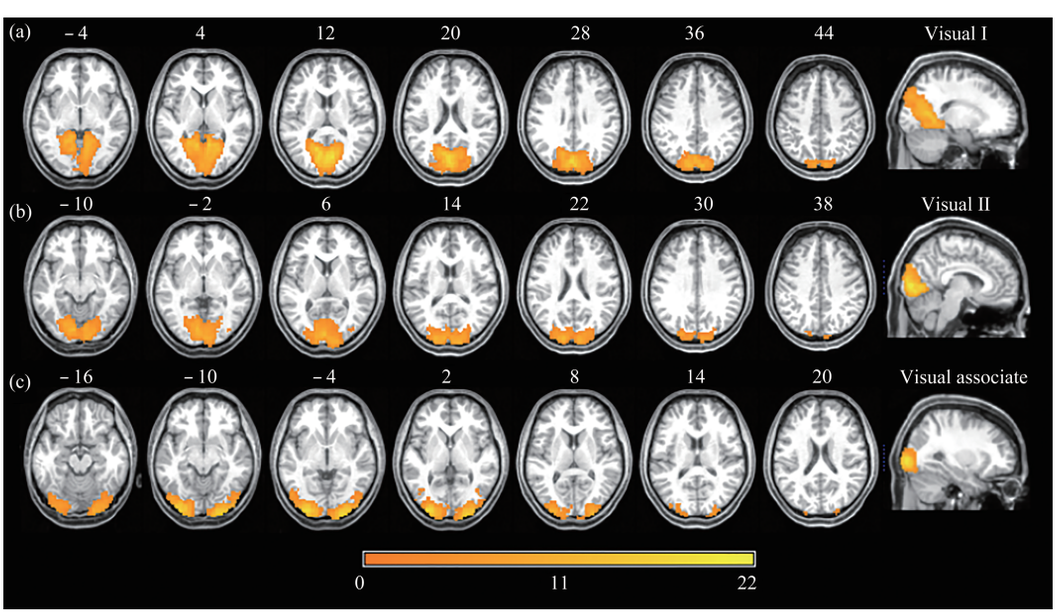



**Fig. 2　Axial sections show visual networks based on TICA**

（a）VisualI area，（b）visualII area，（c）visual association area. Color bar indicates the *Z*-statistic value.

### 1.6　Statistical analysis

The first to the ninth MRI sessions were included in the analysis to assess the effects of SD on vigilance level and spontaneous cerebral activity during the entire 36-h SD procedure. A one-way repeated-measures ANOVA was applied to behavioral data (MRT and LR) from the first to the ninth MRI sessions to assess the alteration of vigilance level. To explore the alteration of neural activity throughout the entire brain, a one-way repeated-measures ANOVA was performed to investigate the effect of SD on ReHo and ALFF maps of the first to the ninth MRI sessions ($P < 0.05$, FWE corrected). A post hoc paired *t*-test with Bonferroni correction was performed to

test differences between the levels. ReHo and ALFF statistical maps were overlapped to extract the brain regions with significant effects on both local functional coherence and low-frequency amplitude. All statistical maps were mapped to the T1-weighted images to facilitate visualization.

To investigate alterations of neural activity within the SMN and VN regions during the entire 36-h SD procedure, the average ReHo and ALFF were calculated for each MRI scan session for each region, which was defined as the average value of ReHo and ALFF among all voxels within the given region. To determine the effects of sleep pressure, circadian rhythm, and their interaction on alterations in neural activity of the SMN and VN regions, 2 × 3 repeated-measures ANOVA was performed on the average values of ReHo and ALFF obtained from each region (sleep pressure state: RW, SD × circadian rhythm: 8:00, 14:00, 20:00) corresponding to the first, second, third, seventh, eighth, and ninth MRI sessions.

To investigate the associations between variation in vigilance level and variation in spontaneous neural activity of the SMN and VN regions during SD, Pearson's correlation coefficients were calculated between MRT and LR variation and ReHo and ALFF variation for each region. MRT and LR variation and ReHo and ALFF variation during SD were defined as the average variation across three contrasts of the 24-h SD procedure (8: 00 contrast, comparing the seventh with the first session; 14: 00 contrast, comparing the eighth with the second session; and 20: 00 contrast, comparing the ninth with the third session).

## 2　Results

### 2.1　Effect of SD on vigilance level

A one-way repeated-measures ANOVA was applied to investigate the alteration of vigilance level in PVT. MRT ($F(8,128) = 12.928$, $P < 0.0001$) and LR ($F(8, 128) = 14.078$, $P < 0.0001$) were both significantly affected during the entire 36-h SD procedure. We considered the first session as the baseline level. For MRT, the fifth ($t(16) = 4.26$, $P < 0.03$), seventh ($t(16) = 4.07$, $P < 0.05$), and eighth ($t(16) = 4.14$, $P < 0.03$) sessions showed significant increases compared with the first session. For LR, the fifth ($t(16) = 3.91$, $P < 0.05$), sixth ($t(16) = 4.15$, $P < 0.03$), seventh ($t(16) = 5.24$, $P < 0.003$), and eighth ($t(16) = 4.51$, $P < 0.02$) sessions showed significant increases compared with the first session (Figure 3).

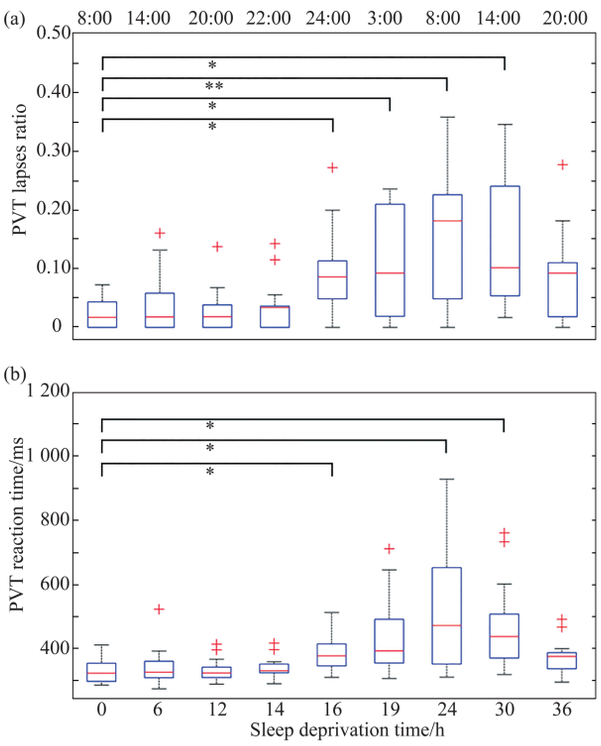



**Fig. 3　Boxplot of PVT behavior measurements**

（a）The PVT lapse ratio（LR）significantly varied across the nine rfMRI sessions（$F$（8，128）= 14.08，$P < 0.0001$）.（b）The PVT mean reaction time （MRT） also significantly varied across the nine rfMRI sessions（$F$（8，128）= 12.93，$P < 0.0001$）. The paired $t$-test results for the comparison between the second to the ninth sessions and baseline （first session） are shown. *$P < 0.05$，**$P < 0.01$.

### 2.2　Effect of SD on ReHo

The results of one-way repeated-measures ANOVA on the ReHo map are shown in Figure 4a. The ReHo map was significantly affected ($P < 0.05$, FWE corrected) during the entire 36 h SD procedure in widespread brain regions, including sensorimotor-related regions (the bilateral precentral gyrus, bilateral postcentral gyrus, bilateral PCL, and bilateral SMA), visual-related regions (the bilateral calcarine gyrus, occipital, bilateral fusiform, and bilateral lingual), round cingulate cortex (the bilateral median cingulate and paracingulate gyrus (PCG), bilateral cuneus, and bilateral precuneus), and other regions (the bilateral rolandic operculum (ROL), bilateral insula, bilateral heschl's gyrus, temporal lobule, and thalamus) (summarized in Table 1). In this study, later region of interest analysis focused on the SMN and VN.

**Table 1 Summary of the brain regions significantly affected by SD on ReHo**

| Brain region | Cluster size | Peak MNI coordinate (*x, y, z*) | Peak *F*-value |
|---|---|---|---|
| Precentral_L | 132 | (−21, −15, 69) | 8.54 |
| Precentral_R | 102 | (45, −12, 39) | 8.21 |
| Rolandic_Oper_L | 101 | (−39, −30, 12) | 9.52 |
| Rolandic_Oper_R | 107 | (36, −24, 18) | 11.33 |
| Supp_Motor_Area_L | 48 | (−3, −18, 54) | 8.33 |
| Supp_Motor_Area_R | 83 | (3, −24, 54) | 8.85 |
| Insula_L | 58 | (−33, −24, 12) | 9.44 |
| Insula_R | 49 | (33, −24, 15) | 11.60 |
| Cingulum_Mid_L | 51 | (−12, −42, 54) | 7.15 |
| Cingulum_Mid_R | 33 | (3, −24, 51) | 8.51 |
| Calcarine_L | 341 | (−18, −69, 18) | 9.12 |
| Calcarine_R | 267 | (12, −84, 3) | 9.21 |
| Cuneus_L | 133 | (−18, −69, 21) | 8.67 |
| Cuneus_R | 99 | (6, −84, 15) | 8.02 |
| Lingual_L | 326 | (−6, −69, 0) | 9.66 |
| Lingual_R | 350 | (9, −75, 0) | 9.23 |
| Occipital_Sup_L | 29 | (−12, −90, 3) | 7.86 |
| Occipital_Mid_L | 113 | (−45, −69, 6) | 7.94 |
| Fusiform_L | 189 | (−30, −63, −12) | 8.49 |
| Fusiform_R | 250 | (27, −72, −6) | 9.12 |
| Postcentral_L | 188 | (−57, −9, 39) | 7.76 |
| Postcentral_R | 198 | (48, −12, 39) | 8.42 |
| Precuneus_L | 70 | (−12, −42, 57) | 8.46 |
| Precuneus_R | 60 | (12, −54, 9) | 7.98 |
| Paracentral_Lobule_L | 77 | (−3, −30, 66) | 8.49 |
| Paracentral_Lobule_R | 36 | (6, −30, 57) | 8.19 |
| Thalamus_L | 54 | (−9, −21, 9) | 7.91 |
| Thalamus_R | 34 | (9, −18, 9) | 6.39 |
| Heschl_L | 57 | (−36, −27, 12) | 10.12 |
| Heschl_R | 52 | (33, −27, 15) | 11.54 |
| Temporal_Sup_L | 218 | (−48, −21, 9) | 9.31 |
| Temporal_Sup_R | 177 | (42, −30, 15) | 8.89 |
| Temporal_Mid_L | 174 | (−48, −66, 6) | 8.11 |
| Temporal_Mid_R | 160 | (45, −57, 9) | 9.14 |
| Temporal_Inf_R | 32 | (45, −51, −24) | 6.88 |

### 2.3 Effect of SD on ALFF

The results of one-way repeated-measures ANOVA on ALFF maps are shown in Figure 4b. The ALFF map was significantly affected ($P < 0.05$, FWE corrected) in widespread brain regions, including the VN (bilateral lingual, bilateral fusiform, and bilateral calcarine gyrus) and other regions (right ROL, right insula, right cuneus, left superior temporal gyrus (STG), and thalamus) (summarized in Table 2).

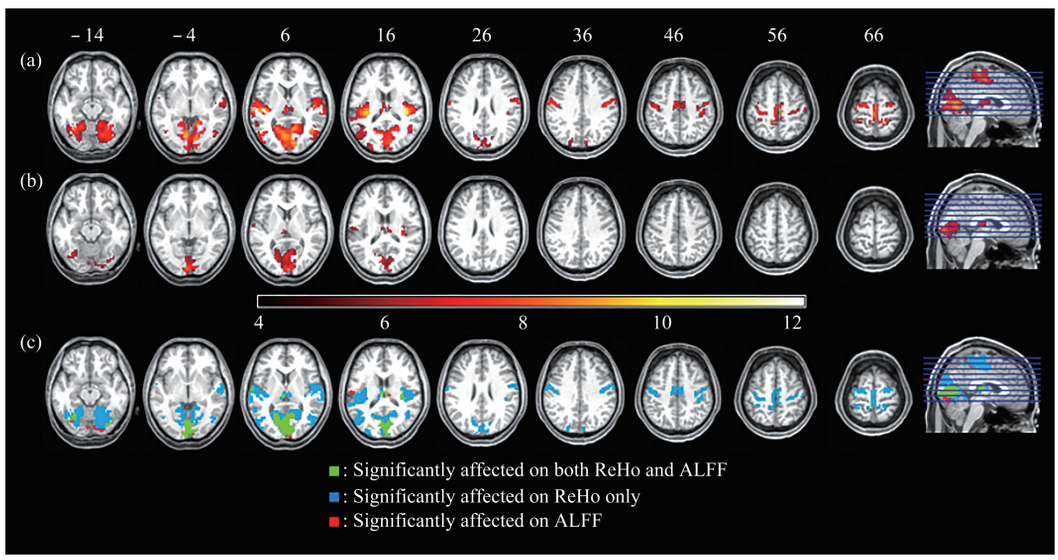



**Fig.4　Axial sections show one−way repeated−measures ANOVA results for ReHo（a）, ALFF（b）, and their overlapping map（c）**

Color bar indicates *F*-values. Blue indicates areas significantly affected on ReHo only，red indicates areas significantly affected on ALFF only，and green indicates areas significantly affected on ReHo and ALFF simultaneously（$P < 0.05$， FWE corrected）. All maps were overlapped on the anatomical template for visualization.

**Table 2 Summary of the brain regions significantly affected by SD on ALFF**

| Brain region | Cluster size | Peak MNI coordinate（MNI space） | Peak *F*-value |
|---|---|---|---|
| Rolandic_Oper_R | 23 | (36, −24, 18) | 7.39 |
| Insula_R | 21 | (33, −24, 18) | 7.44 |
| Calcarine_L | 268 | (0, −90, 0) | 8.40 |
| Calcarine_R | 169 | (6, −90, 3) | 7.88 |
| Cuneus_R | 21 | (6, −93, 15) | 7.11 |
| Lingual_L | 112 | (−6, −84, −6) | 7.13 |
| Lingual_R | 88 | (12, −87, −3) | 7.41 |
| Fusiform_L | 48 | (−33, −66, −15) | 6.51 |
| Fusiform_R | 36 | (42, −69, −18) | 6.57 |
| Thalamus_L | 31 | (−6, −21, 9) | 7.27 |
| Thalamus_R | 21 | (6, −18, 12) | 6.80 |
| Temporal_Sup_L | 18 | (−60, −15, 12) | 6.14 |

## 2.4　Brain regions with both ReHo and ALFF affected

The overlapping map of one-way repeated-measures ANOVA results on ReHo and ALFF is shown in Figure 4c. ReHo and ALFF of visual-related regions (the calcarine gyrus, cuneus, lingual gyrus, and fusiform) were both significantly affected during the entire 36 h SD procedure. However, only ReHo in sensorimotor-related regions (the precentral gyrus, postcentral gyrus, PCL, and SMA) was significantly affected during the entire 36 h SD procedure. In summary, ReHo and ALFF were both affected in the VN (the bilateral lingual, bilateral fusiform, and bilateral calcarine gyri) and other regions (the right ROL, right insula, right cuneus, left STG, and thalamus) during the entire 36 h SD procedure.

## 2.5　Pattern of alteration of neural activities in SMN and VN regions

The average ReHo and ALFF of each SMN and VN region during the entire 36 h SD procedure are shown in Figure 5. The one-way repeated-measures ANOVA results of average values of ReHo and ALFF in each SMN and VN region and the paired *t*-test results between the second to the ninth sessions and baseline (first session) are shown in Tables 3 and 4. All SMN and VN regions were significantly affected ($P < 0.05$) during the entire 36 h SD procedure. Significant variation in ReHo and ALFF mainly occurred in the fifth (24:00, 16 h of SD), sixth (3:00, 19 h of SD), seventh (8:00, 24 h of SD), and eighth (14:00, 30 h of SD) sessions compared with baseline ($t(16) > 3.845$, $P < 0.05$).

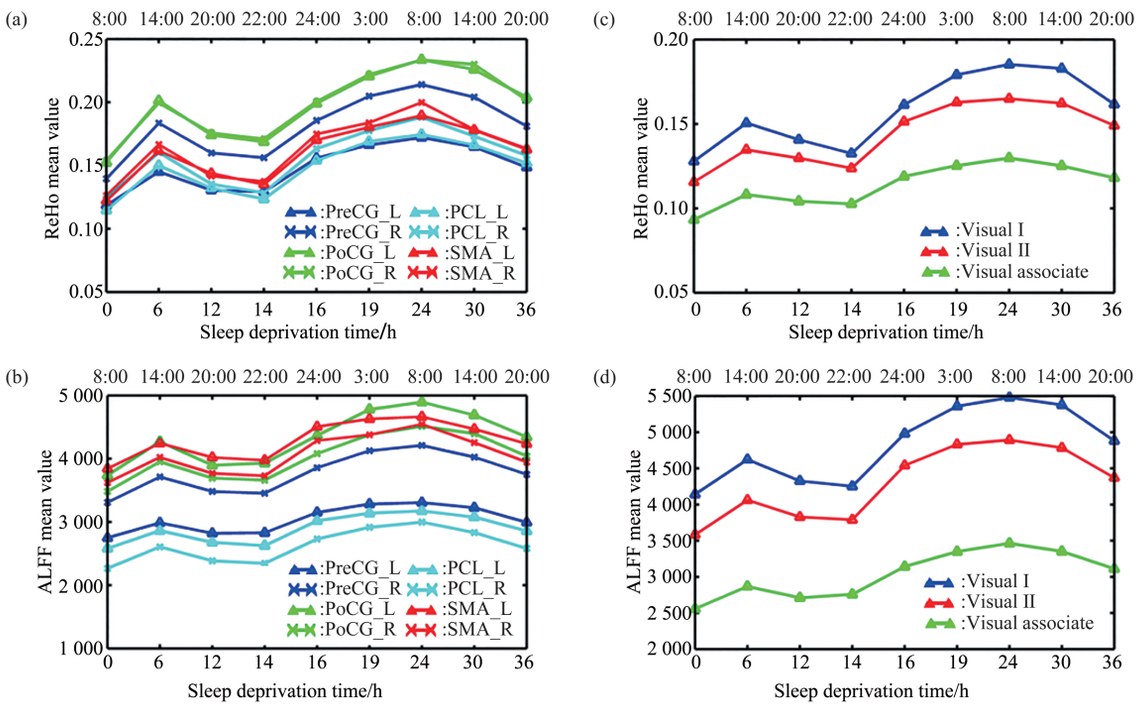



**Fig. 5　Spontaneous neural activity of SMN and VN areas during SD procedure**

(a)Mean ReHo of each SMN area; (b) Mean ALFF of each SMN area;(c) Mean ReHo of each VN area;and (d) Mean ALFF of each VN area. SMN areas include the precentral gyrus(PreCG), postcentral gyrus(PoCG), paracentral lobule(PCL), and SMA extracted from the AAL template. VN areas include the visualI,visual II,and visual association areas extracted from TICA results based on resting state data.

**Table 3　*F*−values of one−way repeated−measures ANOVA on mean ReHo of the first to ninth sessions and *t*−values of paired *t*−test for the difference between the second to ninth sessions and baseline （first session） for each SMN and VN regions**

| Brain region | *F*-value | *t*-value of paired *t*-test | | | | | | | |
|---|---|---|---|---|---|---|---|---|---|
| | | 2nd-1st | 3rd-1st | 4th-1st | 5th-1st | 6th-1st | 7th-1st | 8th-1st | 9th-1st |
| Precentral_L | 13.25*** | 3.39 | 2.61 | 2.32 | 3.93* | 6.15*** | 5.72** | 4.91** | 3.83 |
| Precentral_R | 12.31*** | 4.11* | 3.47 | 2.43 | 4.07* | 6.47*** | 5.74** | 5.21** | 3.64 |
| Postcentral_L | 11.26*** | 4.70** | 3.76 | 2.08 | 3.44 | 6.39** | 5.53** | 5.44** | 4.12* |
| Postcentral_R | 11.95*** | 4.29* | 3.31 | 2.17 | 3.74 | 6.68*** | 5.77** | 5.63** | 3.85* |
| Paracentral_Lobule_L | 11.99*** | 4.15* | 3.56 | 1.64 | 5.04** | 6.56*** | 5.65** | 5.30** | 4.02* |
| Paracentral_Lobule_R | 11.03*** | 3.86* | 1.62 | 0.80 | 3.47 | 6.24*** | 5.39** | 4.63** | 3.45 |
| Supp_Motor_Area_L | 12.35*** | 4.50* | 3.84 | 2.20 | 5.99*** | 6.10*** | 5.83** | 5.40** | 3.87* |
| Supp_Motor_Area_R | 12.92*** | 4.48* | 2.92 | 1.71 | 4.85* | 6.11*** | 5.99** | 4.83** | 3.43 |
| Visual I | 12.86*** | 3.69 | 2.47 | 0.68 | 3.36 | 7.03*** | 5.94** | 6.51*** | 3.28 |
| Visual II | 13.01*** | 3.19 | 2.90 | 1.25 | 4.06* | 8.15*** | 6.14*** | 6.57*** | 3.82 |
| Visual associate | 9.48*** | 2.46 | 3.03 | 2.02 | 3.39 | 7.16*** | 6.05*** | 5.60** | 3.95* |

*$P < 0.05$， **$P < 0.01$， ***$P < 0.001$ （Bonferroni multiple comparison correction）.

**Table 4 *F*−values of one−way repeated−measures ANOVA on mean ALFF of the first to ninth sessions and *t*−values of paired *t*−test for the difference between the second to ninth sessions and baseline （first session） for each SMN and VN regions**

| Brain region | *F*-value | *t*-value of paired *t*-test | | | | | | | |
|---|---|---|---|---|---|---|---|---|---|
| | | 2nd-1st | 3rd-1st | 4th-1st | 5th-1st | 6th-1st | 7th-1st | 8th-1st | 9th-1st |
| Precentral_L | 8.667*** | 2.15 | 1.11 | 1.93 | 3.90* | 5.28** | 4.33* | 4.45* | 2.73 |
| Precentral_R | 8.959*** | 2.86 | 2.19 | 1.50 | 3.76 | 4.86** | 4.96** | 4.07* | 2.82 |
| Postcentral_L | 9.439*** | 3.19 | 1.71 | 2.22 | 3.65 | 5.42** | 4.98** | 4.64* | 3.05 |
| Postcentral_R | 8.592*** | 3.30 | 2.74 | 1.81 | 3.64 | 5.22** | 5.21** | 4.37* | 3.02 |
| Paracentral_Lobule_L | 7.652*** | 2.49 | 1.73 | 0.84 | 5.10** | 5.17** | 4.33* | 4.05* | 2.67 |
| Paracentral_Lobule_R | 8.333*** | 3.33 | 2.38 | 1.22 | 3.65 | 5.44** | 4.59* | 4.41* | 2.92 |
| Supp_Motor_Area_L | 8.445*** | 2.60 | 2.42 | 1.83 | 6.49*** | 5.32** | 4.56* | 4.00* | 3.02 |
| Supp_Motor_Area_R | 8.994*** | 3.04 | 1.92 | 1.53 | 4.44* | 5.91** | 4.79** | 3.60 | 2.37 |
| Visual I | 11.051*** | 2.91 | 1.55 | 0.69 | 3.07 | 5.62** | 5.44** | 5.14** | 3.00 |
| Visual II | 12.809*** | 2.77 | 2.02 | 1.39 | 3.89* | 6.88*** | 6.00** | 5.42** | 3.57 |
| Visual associate | 9.973*** | 2.01 | 1.49 | 1.87 | 3.25 | 6.28*** | 5.66** | 5.10** | 3.63 |

*$P < 0.05$， **$P < 0.01$， ***$P < 0.001$ （Bonferroni multiple comparison correction）.

## 2.6 Effects of sleep pressure， circadian rhythm and their interaction

A significant main effect of sleep pressure on ReHo and ALFF was observed for all SMN and VN regions ($P < 0.001$). A significant effect of circadian rhythm on ReHo was observed for the left precentral gyrus, bilateral postcentral gyrus, right SMA, and left visual I，whereas a significant effect of circadian rhythm on ALFF was observed for the right SMA and left visual I ($P < 0.05$). A significant effect of interaction between sleep pressure and circadian rhythm on ReHo and ALFF was found for all SMN and visual-related areas ($P < 0.05$) (Table 5).

**Table 5 *F*−values of two 2 × 3 repeated−measures ANOVA （sleep pressure × circadian rhythm） on the mean ReHo and ALFF for each SMN and VN regions**

| Brain region | ReHo | | | ALFF | | |
|---|---|---|---|---|---|---|
| | Sleep pressure | Circadian rhythm | Interaction | Sleep pressure | Circadian rhythm | Interaction |
| Precentral_L | 33.496*** | 4.363* | 9.636** | 22.937*** | 3.279 | 4.588* |
| Precentral_R | 26.296** | 3.322 | 9.778** | 18.231*** | 2.348 | 9.607** |
| Postcentral_L | 22.438** | 3.988* | 10.289** | 20.402*** | 2.978 | 7.270** |
| Postcentral_R | 28.642*** | 3.849* | 7.993** | 19.060*** | 2.35 | 10.637** |
| Paracentral_Lobule_L | 24.712*** | 2.456 | 8.900** | 18.185*** | 2.347 | 5.288* |
| Paracentral_Lobule_R | 28.301*** | 3.243 | 6.975** | 20.911*** | 3.096 | 7.511** |
| Supp_Motor_Area_L | 26.301** | 2.739 | 12.325** | 19.187*** | 2.480 | 6.428** |
| Supp_Motor_Area_R | 22.917*** | 4.433* | 12.495** | 16.003*** | 5.067* | 9.426** |
| Visual I | 28.599*** | 3.828* | 7.878** | 25.603*** | 3.816* | 6.112* |
| Visual II | 31.593*** | 2.131 | 9.078** | 30.132*** | 3.063 | 7.321** |
| Visual associate | 25.381*** | 0.867 | 10.289** | 24.100*** | 2.305 | 5.507* |

*$P < 0.05$， **$P < 0.01$， ***$P < 0.001$.

## 2.7 Results of correlation analysis

ReHo variations were significantly positively correlated with MRT and LR variations in brain regions for all SMN regions: the bilateral precentral gyrus (MRT: L/R, $r = 0.51/0.59$, $P < 0.04/0.02$; LR: L/R, $r = 0.61/0.57$, $P < 0.01/0.02$), bilateral postcentral gyrus (MRT: L/R, $r = 0.61/0.57$, $P < 0.01/0.02$; LR: L/R, $r = 0.67/0.58$, $P < 0.01/0.02$), bilateral PCL (MRT: L/R, $r = 0.54/0.60$, $P < 0.03/0.02$; LR: L/R, $r = 0.66/0.72$, $P < 0.01/0.01$), and bilateral SMA (MRT: L/R, $r = 0.61/0.58$, $P < 0.01/0.02$; LR: L/R, $r = 0.67/0.65$, $P < 0.01/0.01$). Visual I (MRT: $r = 0.34$, $P = 0.18$; LR: $r = 0.45$, $P = 0.07$), visual II (MRT: $r = 0.27$, $P = 0.30$; LR: $r = 0.33$, $P = 0.19$), and the visual association area (MRT: $r = 0.44$, $P = 0.08$; LR: $r = 0.43$, $P = 0.09$) did not show significant correlations between ReHo variations and MRT and LR variations (details in Table 6). Scatter diagrams of all SMN regions between ReHo and MRT and LR were drawn for MRT and LR, respectively (Figure 6).

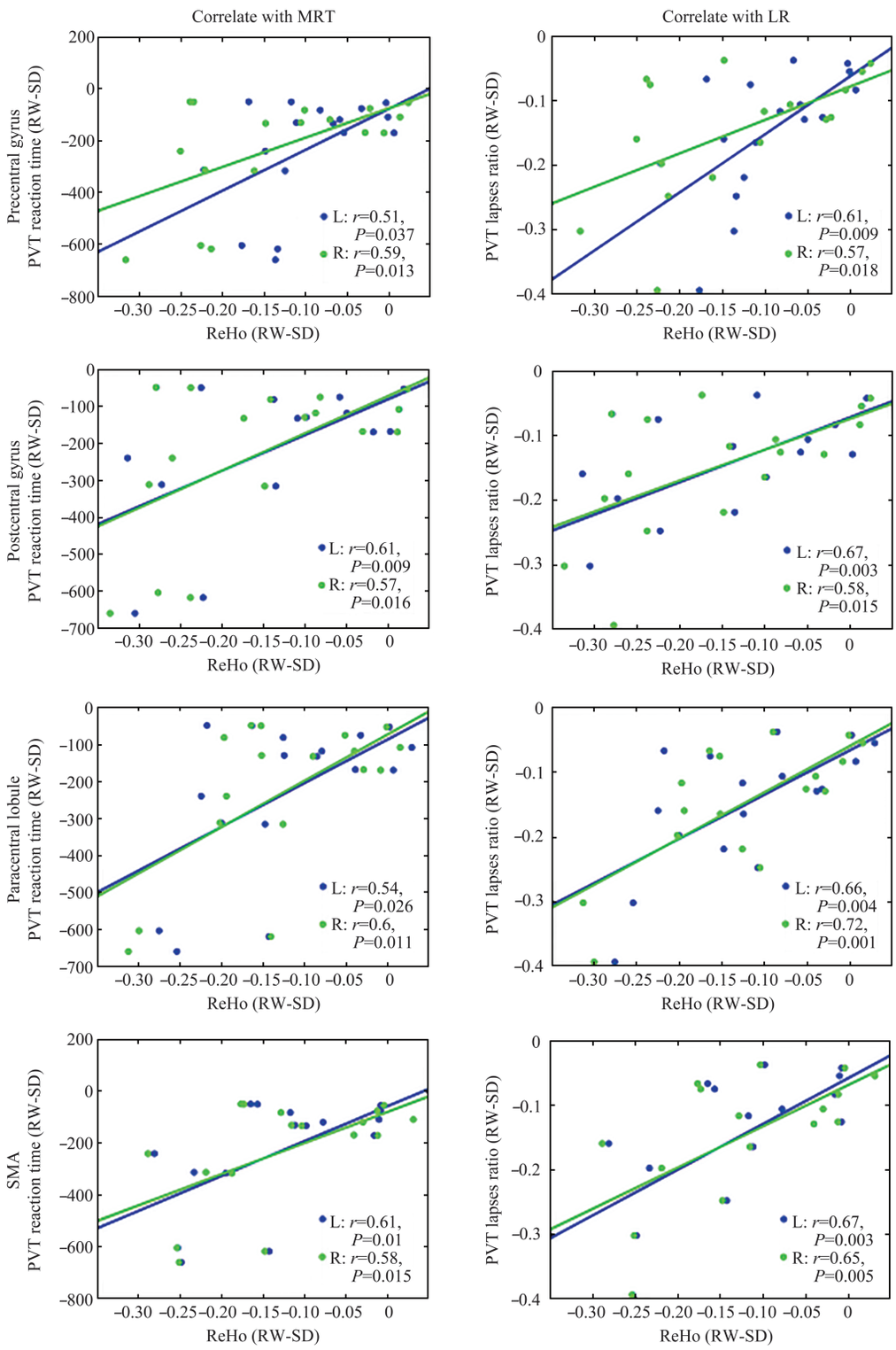



**Fig. 6　Scatter diagrams between ReHo variation and vigilance level variation in SMN areas**

Significant positive correlations between variation of mean reaction time variation (MRT)/lapse ratio (LR) and ReHo variation during SD were observed among eight SMN areas, including the bilateral precentral, postcentral gyrus, paracentral lobule, and SMA. In each scatter diagram, blue indicates left hemisphere results and green indicates right hemisphere results.

**Table 6 Correlation analysis results between ReHo variation and variation in MRT and LR of each SMN and VN regions**

| Brain region | Correlation with MRT | *P*-value | Correlation with LR | *P*-value |
|---|---|---|---|---|
| Precentral_L | 0.51 | 0.037* | 0.61 | 0.009** |
| Precentral_R | 0.59 | 0.016* | 0.57 | 0.018* |
| Postcentral_L | 0.61 | 0.009** | 0.67 | 0.003** |
| Postcentral_R | 0.57 | 0.016* | 0.58 | 0.015* |
| Paracentral_Lobule_L | 0.54 | 0.026* | 0.66 | 0.004** |
| Paracentral_Lobule_R | 0.60 | 0.011* | 0.72 | 0.001** |
| Supp_Motor_Area_L | 0.61 | 0.010* | 0.67 | 0.003** |
| Supp_Motor_Area_R | 0.58 | 0.015* | 0.65 | 0.005** |
| Visual I | 0.34 | 0.182 | 0.45 | 0.070 |
| Visual II | 0.27 | 0.302 | 0.33 | 0.190 |
| Visual associate | 0.44 | 0.081 | 0.43 | 0.088 |

*$P < 0.05$, **$P < 0.01$.

ALFF variations showed significant positive correlation with MRT and LR variations in brain regions for all SMN regions: the bilateral precentral gyrus (MRT: L/R, $r = 0.55/0.53$, $P < 0.03/0.03$; LR: L/R, $r = 0.56/0.57$, $P < 0.02/0.02$), bilateral postcentral gyrus (MRT: L/R, $r = 0.55/0.52$, $P < 0.03/0.04$; LR: L/R, $r = 0.57/0.52$, $P < 0.02/0.03$), bilateral PCL (MRT: L/R, $r = 0.52/0.54$, $P < 0.04/0.03$; LR: L/R, $r = 0.63/0.62$, $P < 0.01/0.02$), and bilateral SMA (MRT: L/R, $r = 0.57/0.52$, $P < 0.02/0.04$; LR: L/R, $r = 0.62/0.58$, $P < 0.01/0.02$. Visual I (MRT: $r = 0.38$, $P = 0.13$; LR: $r = 0.51$, $P < 0.04$) and visual II (MRT: left, $r = 0.45$, $P = 0.07$; LR: $r = 0.52$, $P < 0.04$) showed significant correlations between ALFF variation and LR variation. The visual association area (MRT: left, $r = 0.60$, $P < 0.11$; LR: $r = 0.58$, $P < 0.02$) showed a significant correlation between ALFF variation and MRT and LR variation (Table 7). Scatter diagrams of all SMN regions between ALFF and MRT and LR were drawn for MRT and LR, respectively (Figure 7).

**Table 7 Correlation analysis results between ALFF variation and variation in MRT and LR for each SMN and VN regions**

| Brain region | Correlation with MRT | *P*-value | Correlation with LR | *P*-value |
|---|---|---|---|---|
| Precentral_L | 0.55 | 0.021* | 0.56 | 0.019* |
| Precentral_R | 0.53 | 0.027* | 0.57 | 0.018* |
| Postcentral_L | 0.55 | 0.023* | 0.57 | 0.016* |
| Postcentral_R | 0.52 | 0.032* | 0.52 | 0.032* |
| Paracentral_Lobule_L | 0.52 | 0.032* | 0.63 | 0.006** |
| Paracentral_Lobule_R | 0.54 | 0.026* | 0.62 | 0.008** |
| Supp_Motor_Area_L | 0.57 | 0.016* | 0.62 | 0.008** |
| Supp_Motor_Area_R | 0.52 | 0.031* | 0.58 | 0.014* |
| Visual I | 0.38 | 0.126 | 0.51 | 0.035* |
| Visual II | 0.45 | 0.070 | 0.52 | 0.032* |
| Visual associate | 0.60 | 0.011* | 0.58 | 0.015* |

*$P < 0.05$, **$P < 0.01$.

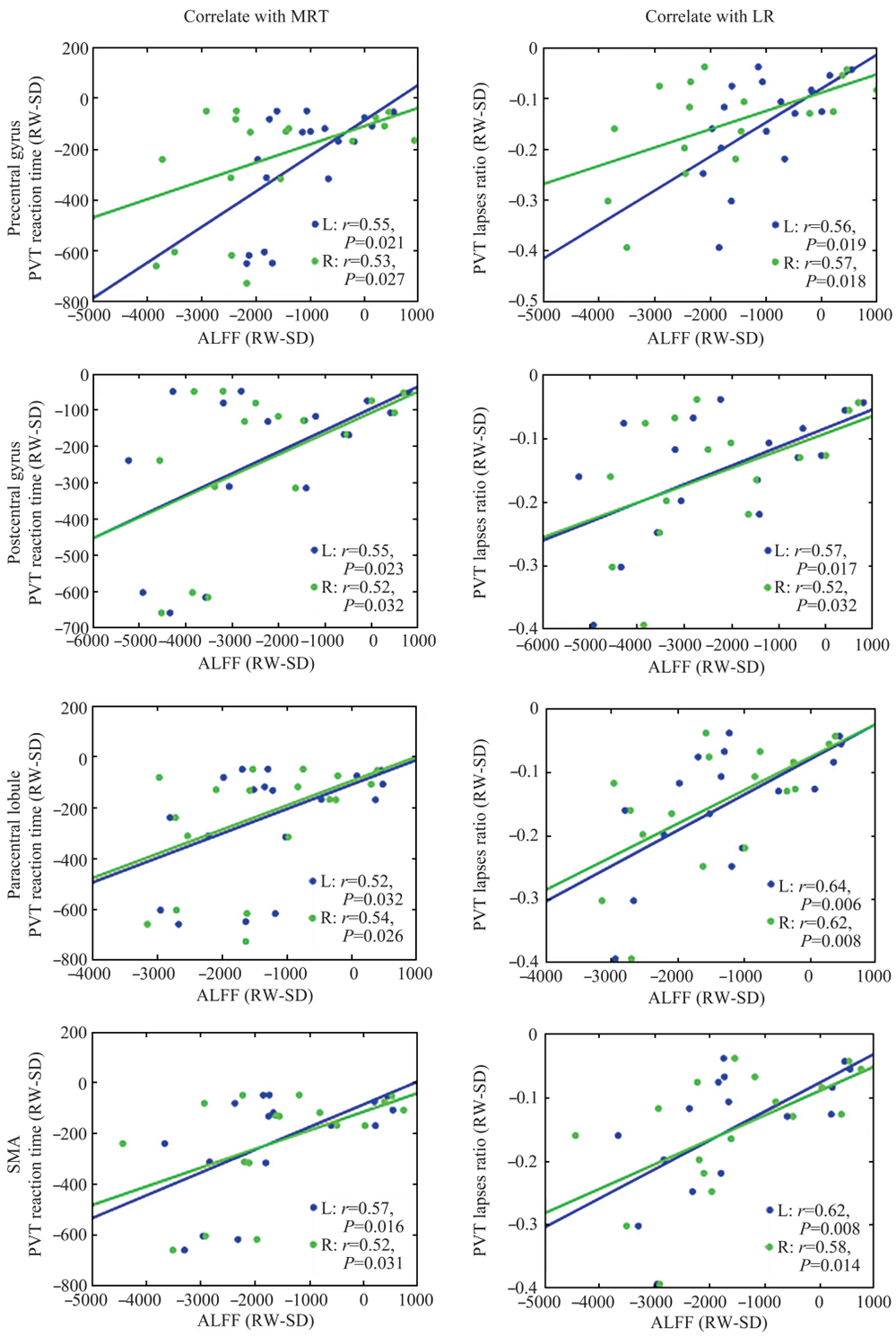



**Fig. 7　Scatter diagrams between ALFF variation and vigilance level variation in SMN areas**

Significant positive correlations between variation of mean reaction time variation (MRT)/lapse ratio (LR) and ALFF variation during SD were found among eight SMN areas, including the bilateral precentral, postcentral gyrus, paracentral lobule, and SMA. In each scatter diagram, blue indicates left hemisphere results and green indicates right hemisphere results.

For each significant result in the correlation analysis, ReHo and ALFF variation exhibited significant positive correlations with MRT and LR variation; similar to the increase in ReHo and ALFF after SD, there was an increase in MRT and LR.

## 3 Discussion

In the present study, we used MRT and LR to measure vigilance level, used ReHo and ALFF to measure spontaneous cerebral activity, and applied one-way repeated-measures ANOVA to explore the alteration of neural activity throughout the entire brain and variations in vigilance level during the entire 36-h SD procedure. The ReHo and ALFF maps were significantly affected in widespread brain regions during SD, particularly in the SMN and VN regions. To elucidate the mechanism of modulation of the sensorimotor and visual cortices during SD, we used 2 × 3 repeated-measures ANOVA (sleep pressure state: RW, SD × circadian rhythm: 8:00, 14:00, 20:00) to assess the effect of circadian rhythm, sleep pressure, and their interaction on the alteration of neural activity of each SMN and VN region. Significant effects of sleep pressure and interaction were observed. To investigate the physiological evidence for decline in vigilance level, we evaluated Pearson's correlation coefficient between MRT and LR variation and ReHo and ALFF variation for each SMN and VN region during SD. All SMN regions exhibited significant correlations between MRT and LR variation and ReHo and ALFF variation.

In the behavioral data, there was a strong effect of SD on MRT ($P < 0.0001$) and LR ($P < 0.0001$), which indicated that vigilance level was highly affected during the entire 36-h SD procedure. As the time progressed, the first significant variations in MRT and LR were observed in the fifth session (24: 00, 16 h of SD) and continued until the eighth session (14: 00, 30 h of SD). Interestingly, this significant variation did not last to the ninth session (20:00, 36 h of SD). These behavioral results were consistent with the spontaneous neural activity of the SMN and VN regions; significant variation compared with baseline occurred primarily in the fifth, sixth, seventh, and eighth sessions, but not in the ninth session. These results suggest that brain neural activity and vigilance level deteriorated mainly during the period from 16 (24: 00) h to 30 (14: 00) h of SD. Previous studies have reported that the sensorimotor and visual cortices were simultaneously affected by sleep debt as well as by circadian rhythm and their interaction[16,18], which is consistent with our result. Melatonin plays an important role in the regulation of sleep-wake cycles [40-41]. It is typically secreted 2 h before the person's regular bedtime and reaches a maximum plasma level around 3 to 4 a. m. [42]. The secretion of melatonin is associated with a person's willingness to sleep and urges the person to enter the normal sleep state. This secretion of melatonin and the disruption of normal sleep may cause alterations of brain neural activity and vigilance level, which were first observed at 24:00.

SD exhibited a significant effect on ReHo and ALFF in widespread brain regions, including the sensorimotor-related regions (the bilateral precentral/ postcentral gyrus, PCL, and SMA), the visual-related regions (the bilateral calcarine gyrus, occipital, fusiform, lingual), the round cingulate cortex (the bilateral DCG, cuneus, precuneus), and other regions (bilateral ROL, insula, heschl's gyrus, STG, and thalamus). These results were consistent with those of previous research [18]. Previous research has indicated that visual information processing and sensorimotor function become less stable and accurate following SD [14], which is consistent with the significant alteration of neural activity in sensorimotor-related and visual-related regions in our study. The DCG, cuneus, and precuneus are nodes in the DMN[43], which plays a pivotal role in higher cognitive processing[44-46], thereby presenting stronger activation in the resting state than in the task state[47]. Our results showed a significant alteration of neural activity in DMN areas. Previous research has reported that the spontaneous activity and connectivity pattern of the DMN were altered following long-term SD[48]. Heschl's gyrus is the first cortical structure to process incoming auditory information[49], and the ROL is an area associated with speech function that is responsible for speech pronunciation and planning[50]. Moreover, our results have indicated that auditory- and speech-related brain neural activity was affected during SD[51-52]. The insula plays an important role in diverse functions that are typically linked to emotion or regulation of the body's homeostasis[53], the thalamus plays an important role in the transitions between sleep and wakefulness[54], which were both significantly affected during the SD procedure[18].

ReHo and ALFF in the SMN and VN both increased during SD. These increases could be considered a manifestation of physiological compensation for brain function during SD[55-56]. The increase of ReHo in the SMN and VN reduced long-range functional connections, resulting in slower response time and more missed trials. The increase of ALFF in the SMN resulted in difficulties in limb control and impulsive behavior. The increase of ALFF in the VN indicated a physiological mechanism to maintain visual fixation tasks during SD. These ReHo and ALFF increase in SMN and VN provide physiological evidence of the slowing of response time during SD.

We found that all SMN and VN regions were significantly affected by sleep pressure and interactions between sleep pressure and circadian rhythm. The SMN and VN regions are typically considered to be simultaneously affected by sleep pressure and circadian rhythm [18]. Our results showed the dominant effect of sleep pressure on the SMN and VN regions rather than a circadian rhythm effect during SD. The significant interaction effect during SD indicates that the circadian rhythm signal was significantly modulated by the sleep pressure.

The SMN regions (the precentral and postcentral gyri, PCL, and SMA) showed significant correlations between MRT and LR variation and ReHo and ALFF variation. This could be attributed to the significant effect of SD on sensorimotor function that complicated the accurate completion of the PVT response in a timely fashion; this finding is consistent with that of a previous study showing that a lesion in the sensorimotor cortex increased the reaction time for the detection of stimulus movements[57-58]. No significant correlations between variation of ReHo and variation of MRT and LR were detected in the visual I, visual II, and visual association areas. Only the visual association area showed a significant correlation between ALFF variation and MRT and LR variation. Previous research has reported that the behavioral response time to a stimulus change can be predicted by neural activity in the advanced visual area (V4) rather than the primary visual area [59], which confirms our results. Our results may imply that the dominance of SMN neural activity variation is confirmed by the decline in vigilance level during SD and that among these three VN regions, the visual association area is responsible for more advanced recognition functions compared with the visual I and II areas, which may be more responsible for the decline in vigilance level. The significant correlation between variation in vigilance level and variation in the neural activity of the SMN may provide physiological evidence for the alteration of vigilance level during SD.

## 4 Conclusion

ReHo and ALFF are useful indices for exploring the alteration of spontaneous cerebral activity during the entire 36 h SD procedure. ReHo and ALFF were significantly affected during the entire 36 h SD procedure in widespread brain regions, particularly in the SMN and VN regions. We observed that brain neural activity and vigilance level deteriorated primarily from 16 to 30 h of the SD procedure, which confirmed the specific time of the occurrence of the SD effect. Moreover, we found a dominant role of the effect of sleep pressure on the SMN and VN regions compared with the circadian rhythm effect during SD and a significant interaction between the effects of sleep pressure and circadian rhythm on neural activity. Our results confirm the dominant role of the effect of SD on the sensorimotor and visual cortices and help us understand the modulatory effect of sleep pressure on the circadian rhythm. Furthermore, we found a significant correlation between variation in the neural activity of the SMN regions and variation in vigilance level during SD, which may provide physiological evidence for the alteration of vigilance level during SD.

**Acknowledgements** We thank YAN Fei, CHEN Qing-Pin, SHI Yuan-Yu, LIU Xue-Ru, GE Yin-Xi, WANG Yun-Xia, ZHOU Li-Qing, and TANG Zhong-Hua for their efforts and assistance for caring for the participants during sleep deprivation. We also thank all the participants of this study.

### References

[1] Aguiar S A, Barela J A. Adaptation of sensorimotor coupling in postural control is impaired by sleep deprivation. Plos One, 2015, **10**(3): e0122340

[2] Sterman M. Effects of sensorimotor EEG feedback training on sleep and clinical manifestations of epilepsy//Biofeedback and Behavior. Springer. 1977: 167-200

[3] Cohen-Zion M, Shabi A, Levy S, *et al*. Effects of partial sleep

deprivation on information processing speed in adolescence. Journal of the International Neuropsychological Society, 2016, **22**(4): 388-398

[4] Stickgold R, James L, Hobson J A. Visual discrimination learning requires sleep after training. Nature Neuroscience, 2000, **3**(12): 1237-1238

[5] Frank M G, Issa N P, Stryker M P. Sleep enhances plasticity in the developing visual cortex. Neuron, 2001, **30**(1): 275-287

[6] Liu Q, Zhou R, Liu L, *et al*. Effects of 72 hours total sleep deprivation on male astronauts' executive functions and emotion. Comprehensive Psychiatry, 2015, **61**: 28-35

[7] Killgore W D, Kahn-Greene E T, Lipizzi E L, *et al*. Sleep deprivation reduces perceived emotional intelligence and constructive thinking skills. Sleep Medicine, 2008, **9**(5): 517-526

[8] Frenda S J, Fenn K M. Sleep less, think worse: the effect of sleep deprivation on working memory. Journal of Applied Research in Memory and Cognition, 2016, **5**(4): 463-469

[9] Chee M W, Choo W C. Functional imaging of working memory after 24 hr of total sleep deprivation. Journal of Neuroscience, 2004, **24**(19): 4560-4567

[10] Roca J, Fuentes L J, Marotta A, *et al*. The effects of sleep deprivation on the attentional functions and vigilance. Acta Psychologica, 2012, **140**(2): 164-176

[11] Lim J, Dinges D F. Sleep deprivation and vigilant attention. Annals of the New York Academy of Sciences, 2008, **1129**(1): 305-322

[12] Nilsson J P, Söderström M, Karlsson a U, *et al*. Less effective executive functioning after one night's sleep deprivation. Journal of Sleep Research, 2005, **14**(1): 1-6

[13] Corsi-Cabrera M, Rosales-Lagarde A. Effects of selective REM sleep deprivation on prefrontal gamma activity and executive functions. International Journal of Psychophysiology, 2015, **96**(2): 115-124

[14] Aguiar S A, Barela J A. Sleep deprivation affects sensorimotor coupling in postural control of young adults. Neuroscience Letters, 2014, **574**: 47-52

[15] Williams G W, Shankar B, Klier E M, *et al*. Sensorimotor and executive function slowing in anesthesiology residents after overnight shifts. Journal of Clinical Anesthesia, 2017, **40**: 110-116

[16] Borb a A, Achermann P. Sleep homeostasis and models of sleep regulation. Journal of Biological Rhythms, 1999, **14**(6): 559-570

[17] Franken P, Dijk D. Circadian clock genes and sleep homeostasis. European Journal of Neuroscience, 2009, **29**(9): 1820-1829

[18] Muto V, Jaspar M, Meyer C, *et al*. Local modulation of human brain responses by circadian rhythmicity and sleep debt. Science, 2016, **353**(6300): 687-690

[19] Biswal B B. Resting state fMRI: a personal history. NeuroImage, 2012, **62**(2): 938-944

[20] Rosazza C, Minati L. Resting-state brain networks: literature review and clinical applications. Neurological Sciences, 2011, **32**(5): 773-785

[21] De Havas J A, Parimal S, Soon C S, *et al*. Sleep deprivation reduces default mode network connectivity and anti-correlation during rest and task performance. NeuroImage, 2012, **59**(2): 1745-1751

[22] Shao Y, Wang L, Ye E, *et al*. Decreased thalamocortical functional connectivity after 36 hours of total sleep deprivation: evidence from resting state FMRI. Plos One, 2013, **8**(10): e78830

[23] Piantoni G, Cheung B L P, Van Veen B D, *et al*. Disrupted directed connectivity along the cingulate cortex determines vigilance after sleep deprivation. NeuroImage, 2013, **79**: 213-222

[24] Goel N, Basner M, Rao H, *et al*. Circadian rhythms, sleep deprivation, and human performance // Progress in Molecular Biology and Translational Science. Elsevier. 2013: 155-190

[25] Habeck C, Rakitin B C, Moeller J, *et al*. An event-related fMRI study of the neurobehavioral impact of sleep deprivation on performance of a delayed-match-to-sample task. Cognitive Brain Research, 2004, **18**(3): 306-321

[26] Zang Y, Jiang T, Lu Y, *et al*. Regional homogeneity approach to fMRI data analysis. NeuroImage, 2004, **22**(1): 394-400

[27] Yang H, Long X-Y, Yang Y, *et al*. Amplitude of low frequency fluctuation within visual areas revealed by resting-state functional MRI. NeuroImage, 2007, **36**(1): 144-152

[28] Lv Y, Margulies D S, Villringer A, *et al*. Effects of finger tapping frequency on regional homogeneity of sensorimotor cortex. Plos One, 2013, **8**(5): e64115

[29] Tian L, Ren J, Zang Y. Regional homogeneity of resting state fMRI signals predicts stop signal task performance. NeuroImage, 2012, **60**(1): 539-544

[30] Chen L, Qi X, Zheng J. Altered regional cortical brain activity in healthy subjects after sleep deprivation: a functional magnetic resonance imaging study. Frontiers in Neurology, 2018, **9**: 588

[31] Dinges D F, Powell J W. Microcomputer analyses of performance on a portable, simple visual RT task during sustained operations. Behavior Research Methods Instruments & Computers, 1985, **17**(6): 652-655

[32] Lim J, Dinges D F. Sleep deprivation and vigilant attention. Ann N Y Acad Sci, 2010, **1129**(1): 305-322

[33] Franzen P L, Siegle G J, Buysse D J. Relationships between affect, vigilance, and sleepiness following sleep deprivation. Journal of Sleep Research, 2008, **17**(1): 34-41

[34] Auerbach E J, Xu J, Yacoub E, *et al*. Multiband accelerated spin-echo echo planar imaging with reduced peak RF power using time-shifted RF pulses. Magnetic Resonance in Medicine, 2013, **69**(5): 1261-1267

[35] Pruim R H R, Mennes M, Van Rooij D, *et al*. ICA-AROMA: A robust ICA-based strategy for removing motion artifacts from fMRI data. NeuroImage, 2015, **112**: 267-277

[36] Yu-Feng Z, Yong H, Chao-Zhe Z, *et al*. Altered baseline brain activity in children with ADHD revealed by resting-state functional MRI. Brain and Development, 2007, **29**(2): 83-91

[37] Tanaka K, Saito H, Fukada Y, *et al*. Coding visual images of objects in the inferotemporal cortex of the macaque monkey. Journal of Neurophysiology, 1991, **66**(1): 170-189

[38] Chenji S, Jha S, Lee D, *et al*. Investigating default mode and sensorimotor network connectivity in amyotrophic lateral

sclerosis. Plos One, 2016, **11**(6): e0157443

[39] Biswal B, Zerrin Yetkin F, Haughton V M, *et al*. Functional connectivity in the motor cortex of resting human brain using echo planar MRI. Magnetic Resonance in Medicine, 1995, **34**(4): 537-541

[40] Emet M, Ozcan H, Ozel L, *et al*. A review of melatonin, its receptors and drugs. The Eurasian Journal of Medicine, 2016, **48**(2): 135-141

[41] Pevet P, Challet E. Melatonin: both master clock output and internal time-giver in the circadian clocks network. Journal of Physiology-Paris, 2011, **105**(4-6): 170-182

[42] Ardura J, Gutierrez R, Andres J, *et al*. Emergence and evolution of the circadian rhythm of melatonin in children. Hormone Research in Paediatrics, 2003, **59**(2): 66-72

[43] Fransson P, Marrelec G. The precuneus/posterior cingulate cortex plays a pivotal role in the default mode network: Evidence from a partial correlation network analysis. NeuroImage, 2008, **42**(3): 1178-1184

[44] Utevsky A V, Smith D V, Huettel S A. Precuneus is a functional core of the default-mode network. Journal of Neuroscience the Official Journal of the Society for Neuroscience, 2014, **34**(3): 932-940

[45] Bush G, Luu P, Posner M I. Cognitive and emotional influences in anterior cingulate cortex. Trends in Cognitive Sciences, 2000, **4**(6): 215-222

[46] Mosebach J, Keilhoff G, Gos T, *et al*. Increased nuclear olig1-expression in the pregenual anterior cingulate white matter of patients with major depression: a regenerative attempt to compensate oligodendrocyte loss?. Journal of Psychiatric Research, 2013, **47**(8): 1069-1079

[47] Brewer J A, Garrison K A, Whitfield-Gabrieli S. What about the "self" is processed in the posterior cingulate cortex?. Frontiers in Human Neuroscience, 2013, **7**: 647

[48] Dai X J, Liu C L, Zhou R L, *et al*. Long-term total sleep deprivation decreases the default spontaneous activity and connectivity pattern in healthy male subjects: a resting-state fMRI study. Neuropsychiatric Disease & Treatment, 2015, 2015(default): **761**-772

[49] Warrier C, Wong P, Penhune V, *et al*. Relating structure to function: Heschl's gyrus and acoustic processing. Journal of Neuroscience, 2009, **29**(1): 61-69

[50] Tonkonogy J, Goodglass H, . Language function, foot of the third frontal gyrus, and rolandic operculum. Archives of Neurology, 1981, **38**(8): 486-490

[51] Glenville M, ., Broughton R, ., Wing a M, *et al*. Effects of sleep deprivation on short duration performance measures compared to the Wilkinson auditory vigilance task. Sleep, 1978, **1**(2): 169-176

[52] Harrison Y, Horne J A. Sleep deprivation affects speech. Sleep, 1997, **20**(10): 871-877

[53] Craig a D, Chen K, Bandy D, *et al*. Thermosensory activation of insular cortex. Nature Neuroscience, 2000, **3**(2): 184-190

[54] Fountoulakis K N, Giannakopoulos P, Kövari E, *et al*. Assessing the role of cingulate cortex in bipolar disorder: Neuropathological, structural and functional imaging data. Brain Research Reviews, 2008, **59**(1): 9-21

[55] Craig A, Tran Y, Wijesuriya N, *et al*. Regional brain wave activity changes associated with fatigue. Psychophysiology, 2012, **49**(4): 574-582

[56] Foxe J J, Morie K P, Laud P J, *et al*. Assessing the effects of caffeine and theanine on the maintenance of vigilance during a sustained attention task. Neuropharmacology, 2012, **62**(7): 2319-2326

[57] Kaneko H, Tamura H, Kawashima T, *et al*. A choice reaction-time task in the rat: a new model using air-puff stimuli and lever-release responses. Behavioural Brain Research, 2006, **174**(1): 151-159

[58] Mohamed M A, Yousem D M, Tekes A, *et al*. Correlation between the amplitude of cortical activation and reaction time: a functional MRI study. American Journal of Roentgenology, 2004, **183**(3): 759-765

[59] Womelsdorf T, Fries P, Mitra P P, *et al*. Gamma-band synchronization in visual cortex predicts speed of change detection. Nature, 2006, **439**(7077): 733-736

# 睡眠剥夺中感觉运动皮层和视觉皮层神经活动及警觉水平的改变*

张　岱[1,2]　左真涛[3,4,5)**]　饶衡毅[6)]　范　勇[7)**]

([1)] 中国科学院自动化研究所模式识别国家重点实验室，北京 100190；

[2)] 中国科学院大学，北京 100049；

[3)] 中国科学院生物物理研究所脑与认知科学统计重点实验室，北京 100101；

[4)] 中国科学院大学中丹学院，北京 100049；

[5)] 中国科学院脑科学与智能技术卓越创新中心，上海 200031；

[6)] *Department of Neurology*, *Perelman School of Medicine*, *University of Pennsylvania*, *Philadelphia*, *PA* 19104, USA）

[7)] *Department of Radiology*, *Perelman School of Medicine*, *University of Pennsylvania*, *Philadelphia*, *PA* 19104, USA）

**摘要**　在睡眠剥夺（sleep deprivation，SD）过程中，人类大脑的神经活动和警觉水平如何受到影响，尤其是感觉运动和视觉系统，目前仍是研究的热点. 静息状态功能磁共振成像（resting state functional magnetic resonance imaging，rfMRI）作为一种反映人脑自发活动的非侵入式成像技术，在睡眠剥夺的研究中得到了广泛应用. 本研究采用9次重复rfMRI和心理运动警觉任务（psychomotor vigilance task，PVT），以探索23名志愿者在整个36 h的睡眠剥夺过程中神经活动和警觉水平的变化. 采用基于PVT的平均反应时间（mean reaction time，MRT）和失效率（lapses ratio，LR）评估警觉水平的变化；采用基于rfMRI的区域同质性（region homogeneity，ReHo）和低频波动幅度（amplitude of low frequency fluctuation，ALFF）评估大脑神经活动变化. 结果表明，感觉运动网络（sensorimotor network，SMN）和视觉区域（visual network，VN）是受到睡眠剥夺影响最严重的区域. 我们采用组独立成分分析（group independent component analysis，GICA）将视觉相关区域划分为视觉I区、视觉II区、视觉关联区，并从解剖自动标记（anatomical automatic labeling，AAL）模板中提取运动感觉相关区域，包括中央前/中央后回、中央旁小叶和辅助运动区. 研究发现，睡眠剥夺后16~30 h脑神经活动及警惕性下降. 采用2×3重复测量方差分析，探讨睡眠压力、昼夜节律及其交互作用对感觉运动相关和视觉相关脑区神经活动的影响. 观察到睡眠压力与交互作用对感觉运动相关区域和视觉相关区域有显著影响. 采用皮尔逊相关系数评估警觉水平变化与感觉运动相关和视觉相关脑区神经活动变化的关系. 睡眠剥夺期间所有感觉运动相关区域的神经活动变化与警觉变化均存在显著的相关关系. 研究结果证实，睡眠剥夺从第一天24:00开始改变SMN和VN的警戒水平和神经活动，睡眠压力和昼夜节律在睡眠剥夺期间调节SMN和VN的神经活动. 此外，昼夜节律的效应受到睡眠压力的显著调节. 感觉运动相关区域和视觉相关区域的增强导致他们远程连接的减弱，这可能是睡眠剥夺期间响应时间变慢的原因.

**关键词**　静息态功能磁共振成像，睡眠剥夺，感觉运动皮层，视觉皮层，大脑神经活动

**中图分类号**　B842.2，R445.2　　**DOI**：10.16476/j.pibb.2019.0055

* 国家重点基础研究发展计划（2015CB856400，2015CB351701），国家自然科学基金（81501158，31730039，31671133），国家重大科学仪器设备开发专项（ZDYZ2015-2）和中国科学院战略重点研究项目（XDBS32000000）资助.

* 通讯联系人.

左真涛. Tel：010-64888462，E-mail：ztzuo@bcslab.ibp.ac.cn

范勇. Tel：0215-7464065，E-mail：yong.fan@ieee.org

收稿日期：2019-03-22，接受日期：2019-04-30